



Effect of AlInGaN barrier layers with various TMGa flows on optoelectronic characteristics of near UV light-emitting diodes grown by atmospheric pressure metalorganic vapor phase epitaxy

Yi-Keng Fu^{a,*}, Yu-Hsuan Lu^{a,b}, Ren-Hao Jiang^{a,c}, Bo-Chun Chen^a, Yen-Hsiang Fang^a, Rong Xuan^{a,d}, Yan-Kuin Su^b, Chia-Feng Lin^c, Jebb-Fang Chen^d

^a Electronics and Optoelectronics Research Laboratories, Industrial Technology Research Institute, Hsinchu, Taiwan

^b Department of Electrical Engineering, Institute of Microelectronics, National Cheng Kung University, Tainan, Taiwan

^c The Department of Materials Science and Engineering, National Chung Hsing University, Taichung, Taiwan

^d Electrophysics Department, National Chiao Tung University, Hsinchu, Taiwan

ARTICLE INFO

Article history:

Received 30 November 2010

Received in revised form 2 March 2011

Accepted 22 April 2011

Available online 13 May 2011

The review of this paper was arranged by Prof. E. Calleja

Keywords:

Quaternary

AlInGaN

Light-emitting diodes

Polarization

Metalorganic vapor phase epitaxy

ABSTRACT

Near ultraviolet light-emitting diodes (LEDs) with quaternary AlInGaN quantum barriers (QBs) are grown by atmospheric pressure metalorganic vapor phase epitaxy. The indium mole fraction of AlInGaN QB could be enhanced as we increased the TMG flow rate. Both the wavelength shift in EL spectra and forward voltage at 20 mA current injection were reduced by using AlInGaN QB. Under 100 mA current injection, the LED output power with $\text{Al}_{0.089}\text{In}_{0.035}\text{Ga}_{0.876}\text{N}$ QB can be enhanced by 15.9%, compared to LED with GaN QB. It should be attributed to a reduction of lattice mismatch induced polarization mismatch in the active layer.

Crown Copyright © 2011 Published by Elsevier Ltd. All rights reserved.

1. Introduction

Recently, tremendous progress has been achieved in GaN-based blue, green and ultraviolet light-emitting diodes (LEDs) [1,2]. Violet LEDs operating 400 nm wavelength is of special interest for solid-state lighting [3]. To achieve a shorter wavelength LED, one needs to reduce the indium composition in the well layers so as to increase its bandgap energy. However, since the QW indium content of near UV LEDs is only a few percent the band offset between QW and (In)GaN quantum barrier (QB) becomes very small leading to poor carrier confinement and low efficiency. Replacing the (In)-GaN barriers by AlGaIn barrier significantly increases the band offset between QWs and barriers resulting in an increased efficiency [4]. However, InGaIn MQWs with AlGaIn barriers are difficult to realize due to the differences between optimal growth conditions for aluminum and those for indium. In addition, the large lattice mismatch between AlGaIn barrier and InGaIn QW can result in

the generation of defects at the AlGaInGaIn interfaces as reported in Ref. [5]. This interface defect may be avoided by using quaternary AlInGaIn interfacial layer [5]. Another important aspect is the effect of the lattice mismatch and the strain between QB and QW on the piezoelectric polarization and the optical properties of the InGaIn MQW active region. AlInGaIn layers can be grown lattice-matched to InGaIn QWs, which in turn can lead to a reduction of the piezoelectric polarization in the QWs [6]. However, to date, the knowledge of optoelectronic characteristics of AlInGaIn/InGaIn MQWs is quite limited partially due to the difficult growth of these heterostructures with device quality.

Recently, Liu et al. have been reported the indium composition of AlInGaIn epilayers increased with increasing growth rate and had good crystalline quality, which does not degrade with increasing growth rate [7]. However, it is not clear the detailed results about AlInGaIn/InGaIn LEDs with various TMGa flows. In this study, we investigated the effect of AlInGaIn barrier layers with various TMGa flows on InGaIn LEDs grown by atmospheric pressure metalorganic vapor phase epitaxy (AP-MOVPE). The optoelectronic characteristics of AlInGaIn/InGaIn near UV LEDs will be demonstrated.

* Corresponding author. Tel.: +886 3 5916951; fax: +886 3 5915138.

E-mail address: YKFu@itri.org.tw (Y.-K. Fu).

2. Experimental procedure

Samples used in this study were all grown on c-face (0 0 0 1) 2 in. sapphire (Al_2O_3) substrates in a atmospheric pressure metalorganic chemical vapor deposition system. During the growth, trimethylaluminum (TMA), trimethylgallium (TMG), trimethylindium (TMI) and ammonia (NH_3) were used as the precursors of Al, Ga, In and N, respectively. Silane (SiH_4) and bicyclopentadienyl magnesium (Cp_2Mg) were used as the n-type and p-type doping source, respectively. Prior to the growth, we heated the substrate to 1100 °C in H_2 ambient to remove surface contamination. We then deposited a 20-nm-thick low-temperature (LT) GaN nucleation layer at 500 °C. After the growth of GaN buffer layers, the temperature was then raised to 1110 °C to grow a 4- μm -thick undoped GaN epitaxial layer with a growth rate of 3.2 $\mu\text{m}/\text{h}$. The 300-nm-thick quaternary AlInGaN layer was subsequently grown on the undoped GaN template at 790 °C using N_2 as the carrier gas. During the growth of AlInGaN layer, we kept the flow rates of TMA, TMI and NH_3 at 0.4 $\mu\text{mol}/\text{min}$, 14.0 $\mu\text{mol}/\text{min}$ and 0.4 mol/min. On the other hand, the TMG flow rates was kept at 10.4, 20.7, 31.1 and 41.4 $\mu\text{mol}/\text{min}$ for sample I, II, III and IV, respectively. We also prepared the AlGaN layer that the TMA, TMG and NH_3 were introduced, labeled as sample V.

Nitride-based LEDs were then fabricated using these various AlInGaN layers. LED structure consists of a 20-nm-thick LT GaN nucleation layer, a 4- μm -thick Si-doped GaN n-cladding layer, an MQW active layer and a 200-nm-thick Mg-doped GaN layer. The MQW active region consists of five periods of 2.4-nm-thick undoped $\text{In}_{0.09}\text{Ga}_{0.91}\text{N}$ well layer and 9-nm-thick undoped AlInGaN barrier layer. We prepared LED I, II and III with the AlInGaN QB grown with an TMG flow of 10.4, 31.1 and 41.4 $\mu\text{mol}/\text{min}$, respectively. The growth time of QB is 568, 175 and 142 s, respectively. For comparison, conventional LED with GaN QB was also prepared, labeled as sample IV. For the fabrication of LEDs, we first partially etched the surface of the samples until the n-type GaN layers were exposed. LEDs with ITO serving as a transparent contact layer (TCL) were fabricated. We subsequently deposited Cr/Au onto the exposed n-type GaN layer to serve as the n-type electrode. The chip size of LEDs was 300 $\mu\text{m} \times 300 \mu\text{m}$. Details of the LED fabrication procedures can be found elsewhere [8,9]. Optical property of the as-grown AlInGaN samples was then evaluated by photoluminescence (PL) using a 25 mW HeCd laser operated at 325 nm as the pumping source. High-resolution double-crystal X-ray diffractometer (DCXRD) was performed to characterize the crystal quality on the Bede D1 system. The X-ray photoelectron spectroscopy (XPS) was also used to determine the amount of aluminum and indium incorporations. Current–voltage (I – V) characteristics of the fabricated devices were then measured at room temperature by an HP4156 semiconductor parameter analyzer. The output powers were measured using the molded LEDs with the integrated sphere detector.

3. Results and discussion

Fig. 1 shows (0 0 0 4) triple-axis $\omega/2\theta$ X-ray diffraction patterns for the five AlInGaN samples with different TMG flow rates. The center peaks at 0 arcsec originate from the underlying GaN layers. For sample V without any indium incorporation, we also observed an AlGaN related peak at the right side of the GaN peaks. The aluminum composition was calculated by 8%. The AlInGaN peak and GaN peak were overlapped together for sample I. It indicated that lattice constant of AlInGaN layer in sample I matched perfectly with the underlying GaN layer. We can also observe clearly that the position of the AlInGaN related peak shifted toward left side as we increased the TMG flow rate during the growth. It should

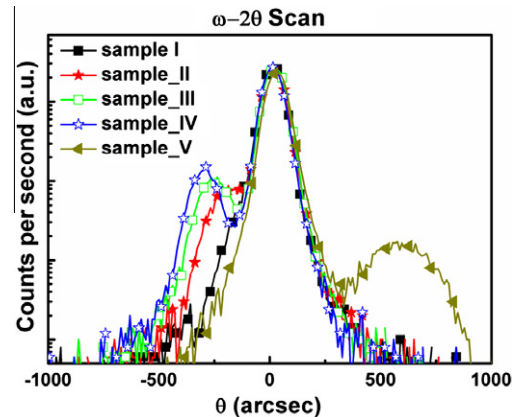


Fig. 1. $\omega/2\theta$ Scan spectra of AlInGaN–GaN heterostructure in the (0 0 0 4) reflection.

be attributed to the increased lattice constant for the AlInGaN with high indium content. On the other hand, the lattice mismatch between QW and QB could be reduced with increasing the TMG flow rate.

Table 1 summarizes XPS and PL results of samples with various TMG flow rates. It was found that the indium content in the AlInGaN layers increased from 1.8% to 3.5% as we increased the TMG flow rate from 10.4 $\mu\text{mol}/\text{min}$ to 41.4 $\mu\text{mol}/\text{min}$. However, it only doubled as we fourfold increased the TMG flow rate. This should be attributed to the saturation of indium incorporation rate at 790 °C in N_2 ambient. We also observed the redshift of PL peak energy because of high indium content. The emission intensity is stronger than that of AlGaN layer (not shown here). The enhanced PL emission is due to the In-segregation effect as reported by other groups [10,11].

Fig. 2 shows I – V characteristics of these four fabricated LEDs. With 20 mA current injection, it was found that forward voltages were 3.17, 3.14, 3.09 and 3.23 V for LED I, II, III and IV, respectively. The forward voltage of LED can be reduced by using AlInGaN QB. Recently, Kuo et al. have been reported the optical properties of InGaN LEDs with low-indium-content InGaN QBs [12]. It was found that the lattice mismatch and corresponding interface charge densities are reduced when the GaN QB are replaced by the $\text{In}_{0.02}\text{Ga}_{0.98}\text{N}$ or $\text{In}_{0.05}\text{Ga}_{0.95}\text{N}$ QBs. The similar results have been reported by Xu et al. [6]. The conduction band on the n -side of the device is approximately the same height as the conduction band on the p -side, which indicates that the polarization-matched active region design minimizes the device force for electrons to leak out of the active region. In this study, the lattice mismatch between QW and QB and corresponding interface charge densities are reduced by increasing In incorporation of AlInGaN QB, which is beneficial for reducing the forward voltage.

Fig. 3 plots the electroluminescence (EL) spectra of these four LEDs at various current injection levels. With 20 mA current injection, it was found that room temperature electroluminescence (EL)

Table 1

Summarized XPS measurement and PL measurement of samples with various TMG flow rates.

Sample	TMGa ($\mu\text{mol}/\text{min}$)	Al composition (%)	In composition (%)	PL peak (nm)
I	10.36	8.9	1.8	357
II	20.71	8.7	2.5	362
III	31.07	9.0	3.0	365
IV	41.43	8.9	3.5	368
V	10.36	7.3	0	342

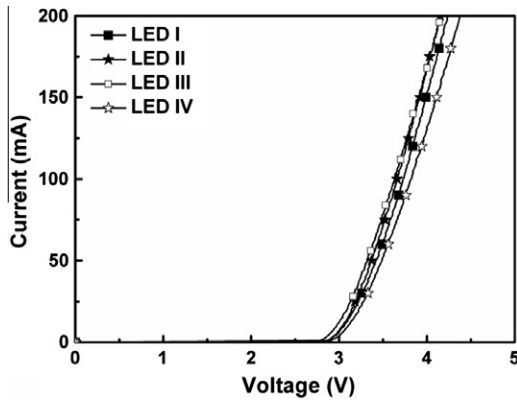


Fig. 2. Forward current–voltage characteristics of these four fabricated LEDs.

peak were 409, 406, 405 and 411 nm for LED I, II, III and IV, respectively. The blueshift wavelength in EL spectra was observed when AlInGa_n QB was used in place of GaN QB. This is due to the AlInGa_n QB can reduce the polarization mismatch and sheet charges. Consistent with a reduction in the sheet charge magnitude, the shift in wavelength with increasing current is also smaller for the AlInGa_n/InGa_n LEDs. As the current is increased from 1 mA to 50 mA, the peak wavelength for the reference LED IV shifts by 3.3 nm; the peak wavelength for the LED I shifts by 1.6 nm. The blueshift of the peak emission wavelength with increasing current is reduced when the indium mole fraction in the AlInGa_n QB increases. The peak emission wavelength is almost independent of the driving current. We can attribute this behavior to the different strengths of piezoelectric fields in InGa_n QWs. Typically, strong

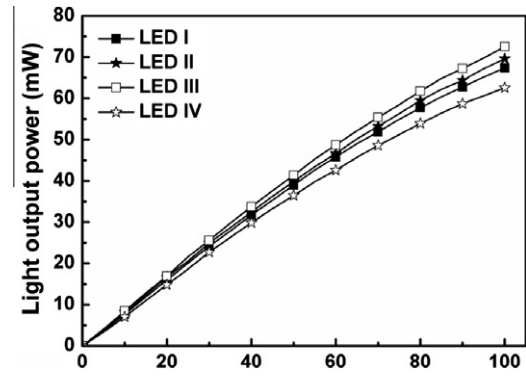


Fig. 4. L – I characteristics of these four fabricated LEDs.

blue-shifts with increasing injection current are observed for QW structure with large piezoelectric field due to the quantum confined Stark effect and the screening of the piezoelectric fields with increasing carrier density [13]. In this study, the lattice mismatch is given by the indium mole fraction in the QWs, which is almost the same (~ 0.09) for all investigated structures, and by the lattice constant of the GaN template layer, which is identical for all samples. There is also no different inhomogeneity of In content. Therefore, the different shifts in the peak emission wavelength are more likely related to the different spontaneous polarizations in the samples. It was attributed to a further reduction in the sheet charge magnitude by increasing indium incorporation of AlInGa_n QB.

Intensity–current (L – I) characteristics of these four fabricated LEDs are also plotted in Fig. 4. It was found that output power of

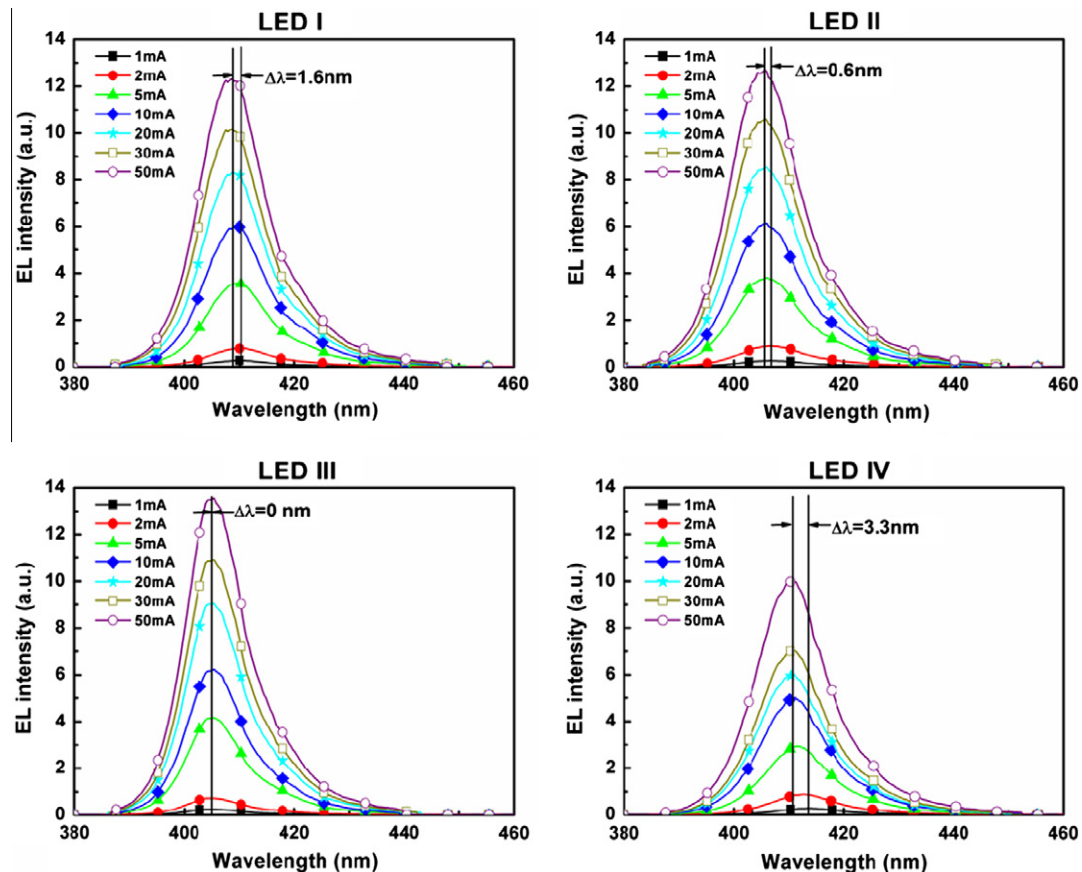


Fig. 3. EL spectra of these three AlInGa_n/InGa_n LEDs and reference GaN/InGa_n LED at various current injection levels.

LEDs with AlInGaN QB was larger than that of LED with GaN QB under the same current injection. With an injection current of 100 mA, the output power were 67.3, 69.6, 72.5 and 62.6 mW for the LED I, II, III and IV, respectively. In other words, the 100 mA output power of LED I can be increased by 7.6% by using AlInGaN QB, compared with LED IV. The slightly larger output power observed from LED I can be attributed to a reduction of lattice constant induced polarization mismatch in the active $\text{In}_{0.09}\text{Ga}_{0.91}\text{N}$ layer. In addition, the output power of AlInGaN/InGaN LEDs could be more enhanced as we increased the TMG flow rate. It was also attributed to the reduced lattice mismatch between QW and QB by increasing indium incorporation of AlInGaN QB. Under 100 mA current injection, the LED III output power can be enhanced by 15.9%, compared with LED IV.

4. Conclusions

In summary, an $\text{Al}_{0.089}\text{In}_{0.018}\text{Ga}_{0.897}\text{N}$ quaternary layer which was lattice-matched to GaN was successful grown. The indium incorporation of AlInGaN layer increases with increasing TMG flow rate. It was found the AlInGaN/InGaN LED can reduce forward voltage, improved light output power by reducing the lattice mismatch induced the polarization mismatch and sheet charges between QW and QB, compared with conventional GaN QB. It also found that the shift in wavelength with increasing current is smaller for the AlInGaN/InGaN LED compared to GaN/InGaN LED. Under 100 mA current injection, the LED output power with $\text{Al}_{0.089}\text{In}_{0.035}\text{Ga}_{0.876}\text{N}$ QB can be enhanced by 15.9%, compared with LED with GaN QB.

References

- [1] Mukai T, Nagahama S, Sano M, Yanamoto T, Morita D, Mitani T, et al. Recent progress of nitride-based light emitting devices. *Phys Status Solidi (a)* 2003;200:52–7.
- [2] Yamada M, Mitani T, Narukawa Y, Shioji S, Niki I, Sonobe S, et al. InGaN-based near-ultraviolet and blue-light-emitting diodes with high external quantum efficiency using a patterned sapphire substrate and a mesh electrode. *Jpn J Appl Phys* 2002;41:L1431–3.
- [3] Narukawa Y, Niki I, Izuno K, Yamada M, Murazki Y, Mukai T. Phosphor-conversion white light emitting diodes using InGaN near-ultraviolet chip. *Jpn J Appl Phys* 2002;41:L371–3.
- [4] Knauer A, Kueller V, Einfeldt S, Hoffmann V, Kolbe T, van Look JR, et al. Influence of the barrier composition on the light output of InGaN multiple-quantum-well ultraviolet light emitting diodes. *Proc SPIE* 2007;6797:67970X1–X6.
- [5] Goto O, Tomiya S, Hohshina Y, Tanaka T, Ohta M, Ohizumi Y, et al. High power pure-blue semiconductor lasers. *Proc SPIE* 2007;6485:64850Z1–Z8.
- [6] Xu J, Schubert MF, Noemaun AN, Zhu D, Kim JK, Schubert EF, et al. Reduction in efficiency droop, forward voltage, ideality factor, and wavelength shift in polarization-matched GaInN/GaN multi-quantum-well light-emitting diodes. *Appl Phys Lett* 2009;94:011113–5.
- [7] Liu JP, Zhang BS, Wu M, Li DB, Zhang JC, Jin RQ, et al. Structural and optical properties of quaternary AlInGaN epilayers grown by MOCVD with various TMGa flows. *J Cryst Growth* 2004;260:388–94.
- [8] Kuo CH, Fu YK, Chi GC, Chang SJ. Efficiency dependence on degree of localization states in GaN-based asymmetric two-step light-emitting diode with a low indium content InGaN shallow step. *IEEE J Quant Electron* 2010;46:391–5.
- [9] Fu YK, Kuo CJ, Tun CJ, Chang LC. Nitride-based blue light-emitting diodes with multiple $\text{Mg}_x\text{N}_y/\text{GaN}$ buffer layers. *Solid-State Electron* 2010;54:590–4.
- [10] Hirayama H, Kinoshita A, Yamabi T, Enomoto Y, Hirata A, Araki T, et al. Marked enhancement of 320–360 nm ultraviolet emission in quaternary $\text{In}_x\text{Al}_y\text{Ga}_{1-x-y}\text{N}$ with In-segregation effect. *Appl Phys Lett* 2002;80:207–9.
- [11] Chen CH, Huang LY, Chen YF, Jiang HX, Lin JY. Mechanism of enhanced luminescence in $\text{In}_x\text{Al}_y\text{Ga}_{1-x-y}\text{N}$ quaternary alloys. *Appl Phys Lett* 2002;80:1397–9.
- [12] Kuo YK, Chang JY, Tsai MC, Yen SH. Advantages of blue InGaN multiple-quantum well light-emitting diodes with InGaN barriers. *Appl Phys Lett* 2009;95:011116–8.
- [13] Li J, Shi SL, Wang YJ, Xu SJ, Zhao DG, Zhu JJ, et al. Violet electroluminescence of AlInGaN–InGaN multiquantum-well light-emitting diodes: quantum-confined Stark effect and heating effect. *IEEE Photon Technol Lett* 2007;19:789–91.